ELSEVIER

Surface and Coatings Technology 98 (1998) 1395–1399

SURFACE & COATINGS TECHNOLOGY

Innovative plasma diagnostics and control of process in reactive low-temperature plasmas

M. Klick [a,*], M. Kammeyer [a], W. Rehak [a], W. Kasper [b], P. Awakowicz [b], G. Franz [c]

[a] *Adolf-Slaby-Institut, Rudower Chaussee 6a, A2489 Berlin, Germany*
[b] *TU München, Lehrstuhl für Technische Elektrophysik, Arcisstr. 21, 80290 Munich, Germany*
[c] *Siemens AG, ZFE T KM 3, 81730 Munich, Germany*

Abstract

By means of two independent diagnostic methods, the plasma parameters in a RIE system (ALCATEL GIR 300) were measured. Density and collision rate of electrons and the power dissipated in the plasma body in He, Ar, O_2, CF_4, and SF_6 were determined.

The first completely new diagnostic method is the self-excited electron plasma resonance spectroscopy (SEERS), which is based on the occurrence of harmonics in the discharge current due to the non-linearity of the sheath at the powered electrode. Owing to the inductive behaviour of the plasma body (bulk, $\epsilon < 0$) and the capacitive nature of the rf sheath, a non-linear and damped series resonance can be observed and used for plasma diagnostics. Its eigenfrequency depends directly on the Langmuir frequency and the electron density, respectively. In order to perform the measurement, the plasma monitoring system HERCULES, containing a robust numerical algorithm, was used.

The second method is a completely automatic Langmuir probe (LP). The compensation of the rf signal was achieved by means of a triaxial setup. The measurement time of one I–V pair takes only 19.5 μs. Retracting the probe tip pneumatically prevents undesirable coating. The I–V curve is smoothed by several FIR-filters to support the automatic calculation of the plasma parameters. Both methods have shown an agreement concerning the electron density and the possibility of advanced process control by innovative plasma diagnostics. © 1998 Elsevier Science S.A.

Keywords: Plasma diagnostics; Low-temperature plasmas

1. Introduction

The application of plasma diagnostics for real processes ensures stability and enables smart process development. This is one of the basic issues of applied plasma physics in the past 20 years. Two innovative and independent diagnostic methods are presented to show the progress in plasma diagnostics. The self-excited electron resonance spectroscopy (SEERS) was developed for use in capacitively coupled rf discharges (RIE, PE, PECVD) and presents volume averaged plasma parameters. This new plasma diagnostic method delivers additional parameters as collision rate and bulk power, which are very helpful in order to verify, scale up and develop plasma processes. In particular, the bulk power is scaling the whole plasma chemistry. The plasma monitoring system HERCULES, including a fast numerical algorithm and a temporal resolution of less than one second, was used to perform SEERS automatically.

The Langmuir Probe (LP) can be used for different discharges and provides local plasma parameters. The LP system used here is a completely automatic Langmuir probe retracting the probe tip pneumatically to prevent undesirable coating.

Langmuir probes allow locally resolved measurements of different plasma parameters besides electron density and ion density. These include plasma potential, floating potential, electron temperature, or the energy distribution function of the electrons. By reason of a non-maxwellian energy distribution of electrons and increased difficulties in electronegative and reactive discharges evaluating the energy distribution, this work is primarily concerned with the comparism of the electron densities measured with both independent diagnostic methods, Langmuir probe and SEERS.

Comparing local and averaged plasma parameters,

* Corresponding author. Tel.: +49 30 6392 5040; fax: +49 30 6392 5041.

PII S0257-8972(97)00261-2

however, requires a sufficiently homogeneous plasma. In order to satisfy this condition and to show that both systems are well suited for real plasma processes, an rf discharge in RIE chamber at low pressure was used.

2. Experimental setup

The commercial RIE system was an Alcatel GIR 300. The chamber comprises a driven substrate electrode and a grounded upper electrode in a cylindrical grounded vessel. The lower electrode was powered at 13.56 MHz. The diameter of the electrodes and chamber was 15.5 cm and 30 cm, respectively. The electrode gap was 6.7 cm.

Commonly used gases were chosen for this work. The experiments were carried out at different pressures in the range of 2–10 Pa. Both diagnostic systems are working basically at higher pressure as well. In the case of higher pressure, the plasma is, depending on the gas, very inhomogeneous, so that local and volume-averaged parameters are no longer comparable or require the determination of the density profile inside the bulk plasma.

The details of the setup are shown in Fig. 1. The sensor for the discharge current measurement (SEERS) and the LP were mounted in KF40 flanges. The probe tip was adjusted to be between the electrodes at a radius of 12 cm and with a distance of 3 cm to the grounded, upper electrode. A tungsten wire with a length of 8 mm and a diameter of 100 μm was used as the probe tip.

3. Diagnostics

The first method, self-excited electron plasma resonance spectroscopy (SEERS), is based on the non-linearity of the space charge sheath (sheath) at the rf electrode, which provides harmonics with the modulated sheath width and high-frequency oscillations in the plasma bulk. Only a brief summary is presented in this paper, and details are described in Refs [1–4].

In order to include the non-linear sheath capacitance, the fundamental relation of the temporal derivative of sheath voltage, u, sheath width, $s[u]$, and displacement current, i [1]:

$$\frac{\mathrm{d}u}{\mathrm{d}t} = \frac{s[u(t)]i(t)}{A_0\epsilon_0} \tag{1}$$

is used and indicates the non-linear properties of the sheath. A_0 denotes the rf electrode area. The degree of non-linearity depends on the ion density distribution within the sheath and results basically in a saw tooth-shaped current [1].

Using a hydrodynamic approach for the electrons, the known equation for the permittivity of the cold plasma can be expressed as:

$$\frac{\epsilon}{\epsilon_0} = 1 - \frac{\omega_e^2}{\omega(\omega - j\nu)}, \quad \omega_e^2 = \frac{e^2 n}{\epsilon_0 m_e}, \tag{2}$$

where ω_e is the electron plasma (Langmuir) frequency. When the collision rate ν vanishes, Eq. (2) is known as the Eccles relation.

Bearing in mind the relation between electrostatic field and current density $J = j\omega\epsilon E$ for $(\omega_e/\omega)^2 \gg 1 + (\nu/\omega)^2$ [1], the conductivity can be written as:

$$\sigma_p = \frac{ne^2}{m_e(j\omega + \nu)} \tag{3}$$

and the potential drop of the bulk plasma in the time domain as

$$u_p = \frac{m_e l}{A_0 n e^2}\left(\nu i + \frac{\mathrm{d}}{\mathrm{d}t} i\right). \tag{4}$$

Neglecting the conduction currents of ions and electrons in the sheath, however, one obtains

$$\frac{\mathrm{d}}{\mathrm{d}t} u_{\mathrm{rf}} + \frac{\bar{s} - s[u(t)]}{A_0\epsilon_0} i = \frac{\bar{s}}{A_0\epsilon_0} i + \frac{m_e l}{A_0 n e^2}\left(\nu \frac{\mathrm{d}}{\mathrm{d}t} i + \frac{\mathrm{d}^2}{\mathrm{d}t^2} i\right) \tag{5}$$

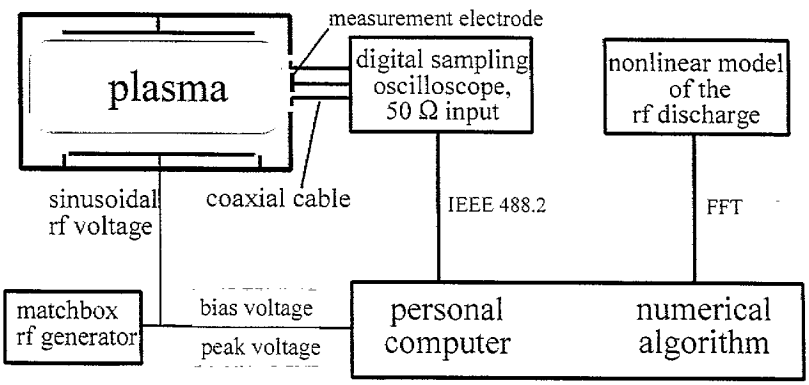

Fig. 1. Experimental setup for SEERS.

for the whole discharge driven by the voltage u_{rf} at the rf electrode [2,4].

This is a non-linear, inhomogeneous, and stiff differential equation of second order. On the right hand side of Eq. (5) is a linear oscillation term with the geometric resonance frequency $\omega_p^2 = \omega_e^2 s/l$ for a plasma with small degree of damping, where l denotes the effective geometric length of the plasma.

The dependence of the sheath width on the displacement current involves a special approach and usually requires a numerical solution of the differential Eq. (5).

This differential equation can be interpreted using an equivalent circuit. On the left hand side, we have the external excitation—the matchbox including the rf generator. The discharge is treated as a damped oscillating circuit as suggested by the right hand side of Eq. (5).

Finally, we have the non-linear phenomenon, given by the second term on the left hand side of Eq. (5). The non-linearity of the sheath (compare with Eq. (1)) provides harmonics exciting the oscillating circuit. This additional resonance can be observed measuring the discharge current. Because of unavoidable stray and feedthrough capacitances at the powered electrode, a direct measurement of the discharge current is very difficult in commercial systems. HERCULES uses a special sensor in a coaxial geometry (50 Ω) inserted into the wall (flange) of the recipient as a virtual part of the wall. By means of the non-linear model, the current pitch ratio of the current measured and the real discharge current can be determined. Therefore, calibration depending on the sensor position is not necessary. An insulating layer on the sensor can be treated as capacitance causing a very small series impedance, which has to be compared with 50 Ω. Therefore, these layers up to a thickness of 100 μm can be neglected.

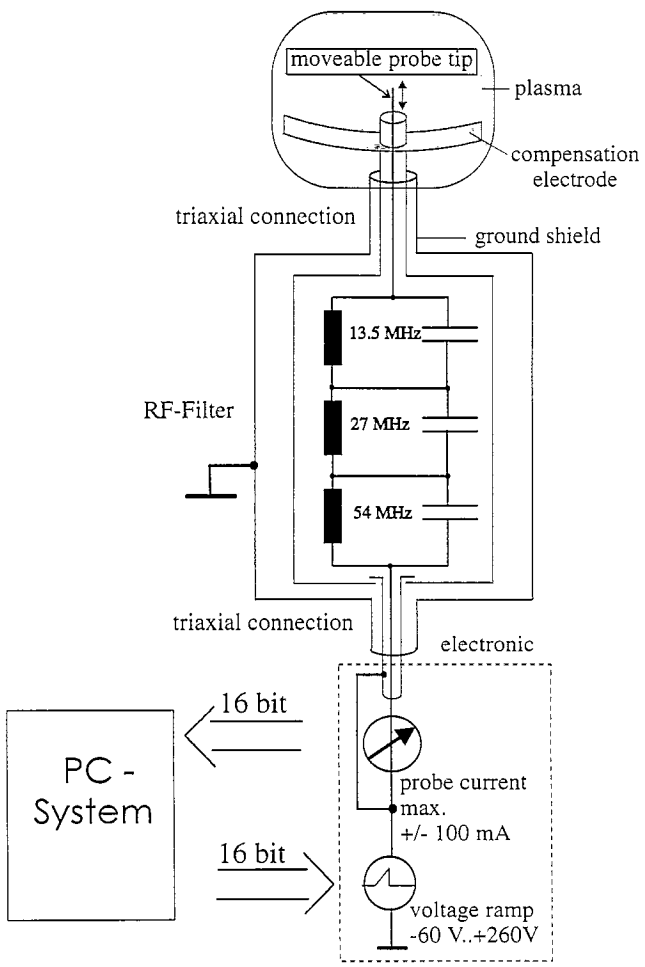

Fig. 2. Experimental setup for Langmuir probe.

The discharge current is detected by a digital sampling oscilloscope with a bandwidth of 500 MHz, and the corresponding parameters are processed by a fast numerical algorithm. Using the differential equation and the measured discharge current, the unknown coefficients can be determined, permitting the calculation of the electron plasma density, the collision frequency, the plasma resistance and the power dissipated in the plasma body.

The second method, a Langmuir probe technique, delivers concentrations of electrons and ions and the electron energy distribution function (EEDF). Since the pioneering work of Langmuir [5], several versions of the probe have been developed. Numerous papers [6–8] have demonstrated the perturbing effects of rf modulation on the single probe characteristic.

In this work, the probe was completely built up using a triaxial technique (Fig. 2) in order to minimize the described capacitive coupling [6] of the feed line. The compensation electrode was extended as an interior shielding [9,10], and it was formed by a V-shaped aluminium strip that was positioned along the plasma confining wall. The probe tip was retracted pneumatically in a capillary tube of quartz glass during the measuring breaks.

The measurement of one I–V-pair requires only 20 μs, ensuring that the probe tip was exposed to the plasma for a short time (0.3 s) only. Contaminations were optionally sputtered by a negative voltage or evaporated applying a positive voltage.

The electronic equipment consists of an automatic measuring system generating a voltage ramp with a maximum range from −60 V to +260 V. The voltage ramp was centred to the floating potential. The probe current was measured in eight different ranges from 31.6 μA to 100 mA full scale.

Before the completely automatic evaluation, the measured I–V-curve was smoothed in the frequency range using filter functions as Gauss and Blackman.

The average electron energy $<E_e>$ can be calculated with three different methods. The slope of the logarithmic electron repelling current is especially reliable in the case of a high plasma density, which is related to a Maxwell distribution with low deficiency in the high

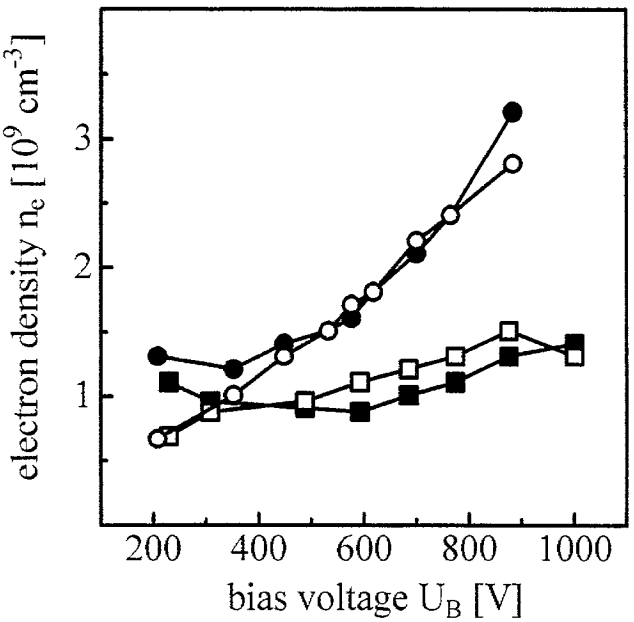

Fig. 3. Electron density n_e (■, ●: SEERS; □, ○: LP) vs. on bias voltage U_B in He at 5 Pa (■, □) and 10 Pa (●, ○).

energy domain. The slope of the second derivative of the electron repelling current in a logarithmic plot shows advantages in the case of low plasma density, often leading to larger deviation from the Maxwell-distribution. The electron density n_e is also calculated by evaluation of the electron saturation current, measuring the current at the plasma potential, and integrating the electron repelling current. The deviation of these three values is typically less than 10%.

4. Results and discussion

For the experiments, the power or the bias voltage, respectively, was varied at different pressures, 2, 5, 10 Pa, for He, Ar, O_2, CF_4, and SF_6. Most measurements were performed at 2 Pa. Mainly, the dependence of the electron density on the bias voltage was determined using SEERS and LP. Both diagnostic methods, SEERS and LP, are independent of the process gas used. The insensitivity to deposited layers and reactive gases of SEERS is due to the underlying physical effect requiring only an rf discharge current sensor measurement using a small and smart sensor in a standard flange. Thus, the rf current sensor had not been cleaned during all experiments, despite contaminations particular in SF_6. The LP system avoids contamination of the probe tip by pneumatically retracting.

Fig. 3 shows the density of electrons, depending on bias voltage in He at 5 and 10 Pa. Unfortunately, at lower pressure, the He discharge was not stable at low

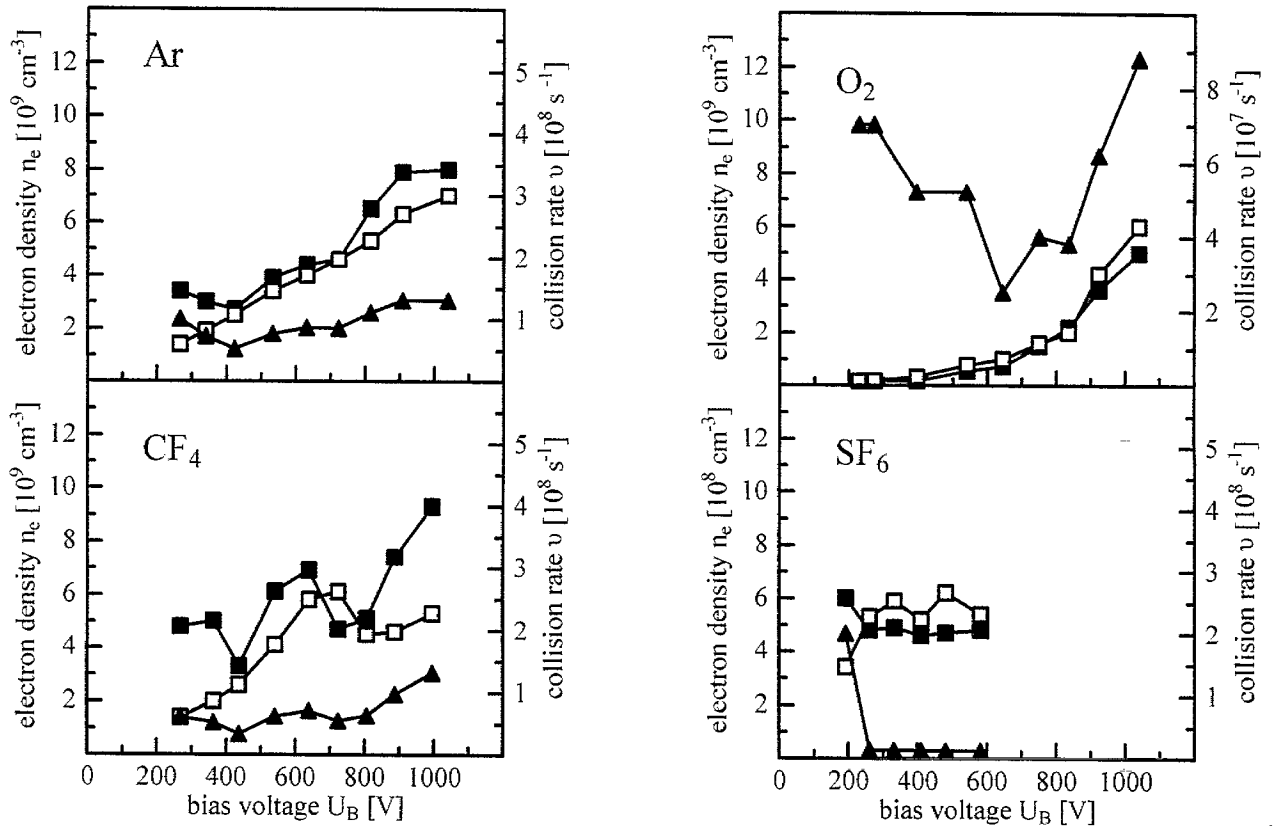

Fig. 4. Electron density n_e (■: SEERS; □: LP) and collision rate ν (▲) vs. on bias voltage U_B in Ar, CF_4, O_2, and SF_6 at 2 Pa.

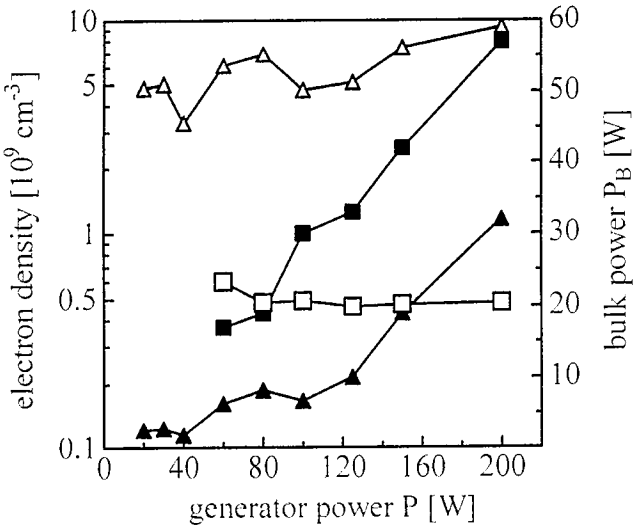

Fig. 5. Electron density n_e (□, △) and bulk power P_B (■, ▲) vs. on generator power P, in SF_6 (▲, △) and CF_4 (■, □) at 2 Pa, measured with SEERS.

power. The results show a good agreement of both methods. The largest deviations were observed for weak discharges where, in particular, the radial profile was changed and the plasma bulk was restricted to the volume between the electrodes. Bearing in mind the volume-averaging of the electron density, n_e, strictly speaking $<n_e^{-1}>^{-1}$, the volume-averaged value (SEERS) should be different for weak discharges ($U_B \leq 300$ V, $P \leq 50$ W) and, depending on gas, for higher pressure.

Fig. 4 shows density and (effective) collision rate of the electrons at 2 Pa. Both independent methods for the electron density provide approximately the same values. The deviation for weak discharges was already discussed for He. The increase of the collision rate for higher voltages has two reasons, the dependence of mobility and collision rate, respectively, on the electric field within the plasma bulk and, as a second order effect, the increase in electron temperature.

In O_2, an excellent agreement was found as well (Fig. 4). In the more complex discharges, as for CF_4 and SF_6, fluctuations of the plasma were observed, resulting in an increased error of both methods. The experiments in CF_4 and SF_6 were performed in the same rf power range. As can be seen in Fig. 4, the relations of bias voltage and electron density are completely different. The well-known reason is the large number of negative ions resulting in a completely different axial density profile in the bulk plasma. Close to the sheath of the driven electrode, a dense and bright plasma range and a sharp decrease of electron temperature and density in the remaining bulk plasma can be observed. Thus, the Bohm criterion had to be modified as well [11–14].

From the density and collision rate of the electrons and the true discharge current, the electronic bulk power can be derived, which is shown in Fig. 5 for SF_6 and CF_4. Based on an acceleration in the d.c. field, the ionic power is not included. The main effect is that the bulk power in SF_6 is about twice that of the CF_4 bulk power at the same rf generator power and lower bias voltage.

For all experiments, the rf peak voltage is approximately equal to the bias voltage (±15%).

5. Conclusions

Despite the restriction to lower pressures for this comparison, both methods have shown a very good agreement regarding the electron density as a key parameter for plasma processing. Both methods are reliable and stable, even in process gases and in a commercial RIE chamber. A forthcoming investigation will be extended to higher pressures, including a determination of the radial and axial profile of electron density in the bulk plasma.

References

[1] M. Klick, J. Appl. Phys. 79 (1996) 3445.
[2] M. Klick, W. Rehak, 12th International Symposium on Plasma Chemistry, Minneapolis, August 1995, University of Minnesota, 1995, Vol. 1, pp. 511–516.
[3] M. Klick, in Proceedings of the 10th International Colloquium on Plasma Processes, French Vacuum Society, Antibes, 1995, p. 341.
[4] M. Klick, Jpn. J. Appl. Phys. 36 (1997) 4625.
[5] I. Langmuir, Collected Works of Irving Langmuir, New York, 1961, Vols 3 and 4.
[6] H. Sabadil, S. Klagge, M. Kammeyer, Plasma Chem. Plasma Process. 8 (1988) 425.
[7] P.A. Chatterton, J.A. Rees, W.L. Wu, K. Al-Assadi, Vacuum 42 (1991) 489.
[8] B.A. Annaratone, N.St.J. Braithwaite, Meas. Sci. Technol. 2 (1991) 795.
[9] W. Kasper, H. Böhm, B. Hirschauer, J. Appl. Phys. 71 (1992) 4168.
[10] W. Kasper, ICPIG XXIII (1985), 171.
[11] G. Oelerich-Hill, I. Pakropski, M. Kujawaka, J. Phys. D: Appl. Phys. 24 (1991) 593.
[12] A.P. Paranjpe, J.P. McVitte, S.A. Self, J. Appl. Phys. 67 (1990) 6718.
[13] J. Meichsner, H.U. Poll, K.H. Wickleder, Contrib. Plasma Phys. 25 (1989) 503.
[14] L.G. Christophorou, Contrib. Plasma Phys. 27 (1985) 4237.